

$\Delta^*$ , path traversed by the isotherm under consideration, measured from the fixed surface;  $\tau_\xi$ , time determining the reference point of intersection of the dependence of the path traversed by the isotherm under consideration with the axis of abscissas;  $K$ , temperature coefficient;  $a$ , thermal diffusivity;  $\theta^* = (T^* - T_0)/(T_w - T_0)$ , where  $T_w$ ,  $T^*$ , are the temperatures of the surface of the material and of the isotherm under consideration, respectively;  $T_0$ , temperature of the unheated material;  $\tau_y$ , temperature of the onset of linear entrainment;  $V_\infty$ ,  $V_{0*}$ , speeds with which the outer surface and the isotherm, respectively, move;  $\bar{V}_\infty$ , quasisteady speed with which the surface moves;  $V_{Ty}(\tau_y)$ , speed of the isotherm corresponding to the temperature of onset of linear entrainment at the instant  $\tau_y$ ;  $(\alpha/c_p)_0$ , heat-transfer coefficient;  $K_{Tp}$ , constant of destruction of the material;  $q$ , supplied heat flux;  $q'_{av}$ , mean integral heat flux in the time from 0 to  $\tau_T$ ;  $\lambda$ , thermal conductivity;  $\rho$ , density;  $c$ , heat capacity;  $S$ , linear entrainment;  $S_v$ , linear entrainment at the instant  $\tau_v$ .

#### LITERATURE CITED

1. G. A. Frolov, Yu. V. Polezhaev, V. V. Pasichnyi, and F. I. Zakharov, *Inzh.-Fiz. Zh.*, 40, No. 4, 608-614 (1981).
2. Yu. V. Polezhaev and G. A. Frolov, *Inzh.-Fiz. Zh.*, 50, No. 2, 236-240 (1986).
3. G. A. Frolov, A. A. Korol', V. V. Pasichnyi, et al., *Inzh.-Fiz. Zh.*, 51, No. 6 (1986).
4. Yu. V. Polezhaev and F. B. Yurevich, *Heat Protection [in Russian]*, Moscow (1976).
5. G. A. Frolov, *Inzh.-Fiz. Zh.*, 50, No. 4, 629-635 (1986).
6. G. A. Frolov, V. V. Pasichnyi, Yu. V. Polezhaev, et al., *Inzh.-Fiz. Zh.*, 50, No. 5, 709-718 (1986).
7. M. C. Adams, W. E. Powers, and S. Georgiev, *JAAS*, 27, No. 7, 535 (1960).

#### STUDY OF THE PARAMETERS OF A TWO-PHASE JET AND ITS EFFECT ON A BARRIER

A. P. Iskrenkov, V. V. Mazak,  
M. S. Tret'yak, and V. V. Chuprasov

UDC 532.5

Experimental and theoretical results are presented from a study of the parameters of a high-temperature two-phase jet and its thermal effect on a nonpermeable surface.

The intensive development of technology is associated with an increase in the thermodynamic parameters of the working parts of various devices and, as a rule, with the action of high-temperature multiphase flows (gas-solid-particle and gas-liquid-particle systems, etc.) on the material of structural elements of turbines, rocket engines, plasma chemical reactors, and other power plants operating in high-speed two-phase flows.

In connection with this, it is of great practical interest to study the parameters of two-phase, high-temperature, high-speed flows and their thermal effect on an impermeable surface with different angles of incidence.

To conduct experimental studies, we developed a stand (Fig. 1) which includes an electric-arc gas heater (plasmatron) 1 with a linear design and a nozzle 28 mm in diameter, a batching device for the powdered materials 2, a system 4 to insert and remove the baffle 5 in front of the 40-mm-diameter model 6, an ISSO-1 rate meter 3, an RFK-5 photographic recorder 8, and an EOP-66 pyrometer 9.

The linear plasmatron is distinguished from other types of arc heaters by the simplicity of its design and the convenience of its use. The plasmatron was described in detail in [1] along with results of study of its thermal and electrical characteristics for air, nitrogen, and carbon dioxide.

---

A. V. Lykov Institute of Heat and Mass Transfer, Academy of Sciences of the Belorussian SSR, Minsk. Translated from *Inzhenerno-Fizicheskii Zhurnal*, Vol. 52, No. 1, pp. 37-42, January, 1987. Original article submitted November 14, 1985.

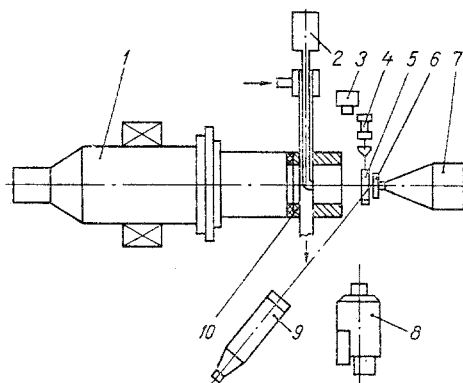


Fig. 1. Diagram of test stand: 1) electric-arc plasma generator; 2) solid-particle batcher; 3) ISSO meter to measure velocity of luminous objects; 4) air cylinder; 5) baffle; 6) test model; 7) holder; 8) RFK-5 photographic recorder; 9) ÉOP-66 pyrometer; 10) water-cooled nozzle.

The system for introducing the model into the plasma flow is controlled automatically or manually (remotely) from a control panel and contains a holder 7, allowing a change in the angle of inclination of the model from 0 to 90°, an uncooled copper baffle 5 brought into motion by an air cylinder 4, and an electromechanical circuit with limit switches on the baffle drive and a timer.

The ISSO-1 rate meter (developed by the special design office of the Institute of Physics of the Belorussian Academy of Sciences) is designed to determine the velocity of discrete luminous plasma flows and heated particles in high-temperature jets. The meter operates on the principle of comparison of the velocities of the test object and a standard object. This is done by scanning the image of the trajectory of the object perpendicular to its direction with a mirror which rotates with a known speed. The range of velocity measurement, accurate to within  $\pm 5\%$ , is 6-780 m/sec when done visually and 10-1300 m/sec when done photographically.

The batching device shown in Fig. 2 was developed to feed powdered materials into a plasma flow [2]. It consists of a body 1 enclosing a rotating shaft 2, with a transport disk 3 with holes 4 rigidly attached to the shaft. The body is provided with inlet channels 5 for delivery of the working gas. Located under the disk 3 is the cover of a hopper 6 with ports and outlet channels 7. Channels 5 and 7 are located in the same section. An impeller 8 is installed on the shaft directly under the hopper cover. The lower part of the cylindrical hopper contains a plunger 9.

The powders are batched by changing the volume flow rate of the material through regulation of the velocity of the plunger 9. The powder is forced into the holes 4 in the disk 3, fed by the latter into the channel 7, and transported by the gas into the plasma flow.

We used the above-described stand to experimentally study the effect of a two-phase plasma jet on the heat flow to an impermeable surface. As the solid phase we used polydisperse particles of  $\text{Al}_2\text{O}_3$ , with a 27% (by wt.) feed of this material into the plasma flow. The particles were fed through an opening made axisymmetrically in a special nozzle 10 (Fig. 1) ahead of the electrode-anode. The hole is located 30 mm in front of the edge of the nozzle. Figure 3a shows a histogram of the particle size distribution.

The velocity of the particle-carrier-gas at the outlet was 125 m/sec, while the outgoing flow was axial. Evaluation of the two-phase flow regime shows that a regime of flow of "single" particles was realized (the volume concentration of particles  $\sim 0.005$ ) [3].

The heat flux from the plasma jet to the impermeable surface was determined by an exponential method based on the smallness of the Biot criterion [4].

Figure 3b (curves 1 and 2) shows results of determination of the heat flux acting on a sensor placed on the axis of the model at different distances from the edge of the plasmatron nozzle. The model was 40 mm in diameter. It is evident from the figure that the heat flux from a one-phase plasma jet decreases from  $700 \cdot 10^4$  to  $190 \cdot 10^4$  W/m<sup>2</sup> with an increase in the distance from 75 to 200 mm and decreases from  $965 \cdot 10^4$  to  $250 \cdot 10^4$  W/m<sup>2</sup> for a plasma flow with additions of  $\text{Al}_2\text{O}_3$  particles.

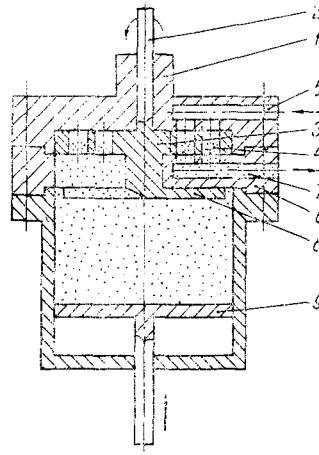


Fig. 2. Batching device for powdered materials.

The substantial increase in heat flux toward the barrier in the two-phase plasma jet is connected in general with processes of contact heat transfer, the conversion of the kinetic energy of the particles into thermal energy, etc. In this case, the contribution of the kinetic energy of the particles to the heat flux is negligible at a distance of 100 mm from the nozzle edge and amounts to no more than  $20 \cdot 10^4$  W/m<sup>2</sup> (about 10% of the increment in heat flux). With an increase in the distance, the velocity of the particles and, accordingly, their kinetic energy decrease, and their effect on heat flow is manifest mainly through contact heat transfer, agitation of the boundary layer, etc.

Figure 3b (curves 3 and 4) shows results of study of the heating effect of a plasma jet with different angles of incidence on the surface of the model. It is evident from the data that with a change in this angle from 30 to 90°, heat flux from a one-phase plasma jet changes by about a factor of 1.5, while heat flux from a two-phase plasma jet changes by a factor of 1.8.

Figures 4 and 5 show results of calculation of the velocity and temperature of particles along the jet axis.

The velocity and temperature of the disperse phase were determined from formulas in [3]:

$$\frac{dU_p(x)}{dx} = \frac{3}{8} \frac{\gamma_g(x) C_D(x) |U_g(x) - U_p(x)| |U_g(x) - U_p(x)|}{U_p \gamma_p r_p}, \quad (1)$$

where

$$C_D(x) = \left[ 0,4 + \frac{4}{\sqrt{\text{Re}(x)}} + \frac{24}{\text{Re}(x)} \right] \left[ 1 + \exp\left(-\frac{0,427}{M_p^{4,63}(x)}\right) \right];$$

$$\text{Re}(x) = \frac{\gamma_g(T^*) 2r_p |U_g(x) - U_p(x)|}{\mu_g(T^*)}; \quad \mu_g(T) = \mu_{av} \left( \frac{T(x)}{T_{av}} \right)^{0,75};$$

$$T^*(x) = \frac{T_g(x) + T_p(x)}{2}; \quad M_p(x) = \frac{|U_g(x) - U_p(x)|}{a_{av} \sqrt{\frac{T_g(x)}{T_{av}}}}; \quad (2)$$

$$\frac{dT_p(x)}{dx} = \frac{3}{\gamma_p c_p r_p U_p(x)} [\alpha(x) (T_g(x) - T_p(x)) - \epsilon \sigma T_p^4],$$

here

$$\alpha(x) = \frac{\text{Nu} \lambda_g(T^*)}{2r_p}; \quad \text{Nu} = \text{Nu}' \left/ \left( 1 + 3,42 M_p(x) \frac{\text{Nu}'}{\text{Re}(x) \text{Pr}} \right) \right.;$$

$$\text{Nu}' = 2 + 0,459 \text{Re}^{0,55}(x) \text{Pr}^{0,33}.$$

In calculating the temperature of the disperse phase, we examined the stage of heating of the particles to the melting point, melting at constant temperature, and subsequent heating or cooling in relation to the heat supplied to the particles by the gas phase.

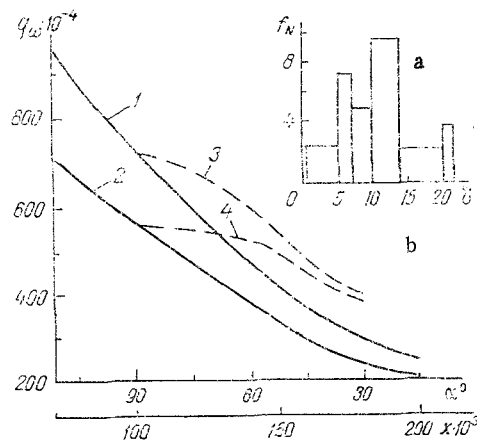


Fig. 3. Histogram of particle size distribution (a) and the dependence of the heat flux on the distance to the edge of the plasmatron nozzle and the angle of incidence of the plasma jet on the surface of the model (curves 1 and 3 are for a two-phase flow; 2 and 4 are for a one-phase flow) (b).

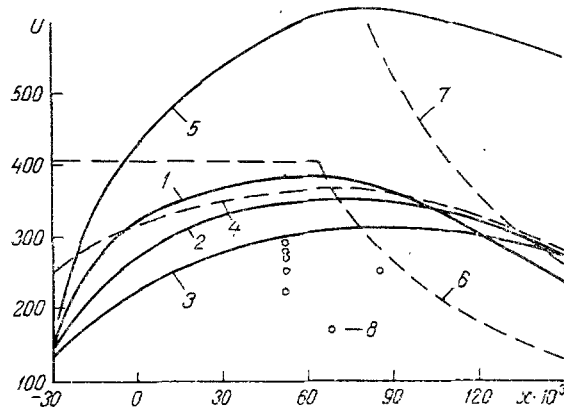


Fig. 4. Distribution of particle and gas velocities along the jet axis:  $U_{p0} = 125$  m/sec,  $U_{g0} = 400$  m/sec,  $r_p = 5 \mu\text{m}$ ; 2) 125, 400, and 7; 3) 125, 400, and 10; 4) 250, 400, and 7; 5) 125, 800, and 7; 6)  $U_g(x)$  at  $U_{g0} = 400$  m/sec; 7) same at 800; 9) experimental values of particle velocity.

The effect of the particles on the gas phase was not considered, while the distribution of gas velocity and temperature along the axis of the turbulent jet were calculated from relations in [5]:

$$\frac{U_g(x)}{U_{g0}} = \frac{0,44}{\left[0,07 \left(\frac{x}{r_0}\right) + 0,29\right]^2} \quad \text{at } \frac{x}{r_0} > 5,33;$$

$$\frac{T - T_\infty}{T_g - T_\infty} = \frac{0,3}{\left[0,07 \left(\frac{x}{r_0}\right) + 0,29\right]^2} \quad \text{at } \frac{x}{r_0} > 3,68,$$

which were validated by experimental data obtained on the above-described test stand [6].

The system of equations was solved by a fourth-order Runge-Kutta method. The calculations were performed on a microcomputer.

It can be seen from Fig. 4 that the experimental values of particle velocity are below the theoretical values. This is probably related to the fact that we used the gas velocity for a one-phase jet in the calculations. At the same time, the dynamic head 75-200 mm from the nozzle edge in the two-phase flow is 0.85 of the dynamic head in the one-phase flow, while the velocity of the gas in the jet in the presence of a disperse phase decreases in

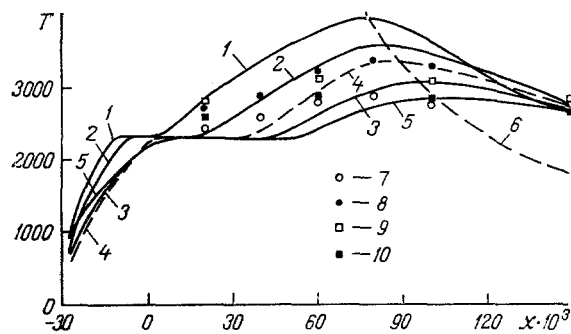


Fig. 5. Distribution of particle and gas temperature along the jet axis: 1)  $U_{p0} = 125$  m/sec,  $U_{g0} = 400$  m/sec,  $r_p = 5$   $\mu$ m; 2) 125, 400, and 7; 3) 125, 400, and 10; 4) 250, 400, and 7; 5) 125, 800, and 7; 6)  $T_g(x)$  at  $U_{g0} = 800$  m/sec. Experimental data on color temperature: 7)  $\epsilon_{0.53}/\epsilon_{0.66} = 2$ , 8)  $\epsilon_{0.53}/\epsilon_{0.66} = 1.5$ ; on brightness temperature: 9)  $\epsilon = \epsilon(T = 2300^\circ\text{K})$ , 10)  $\epsilon = \epsilon(T = 2700^\circ\text{K})$ .

the above-described case by about 15% both as a result of particle momentum transfer and an increase in density due to the temperature decrease.

A twofold change in particle diameter (curves 1 and 3, Fig. 4) does not lead to a significant change in particle velocity. This finding is consistent with the experimental results in [3]. A twofold increase in the velocity of particles entering the plasma jet (curves 2, 4) also only slightly changes particle velocity in the flow. At the same time, an increase in flow velocity by a factor of two leads to an increase in particle velocity by a factor of about 1.8 (curves 2, 5), while particle temperature decreases by about  $700^\circ\text{C}$  (curves 2 and 5, Fig. 5) due to a shortening of the time the particles are in the flow.

The beginning and end of melting of the disperse phase and the distance at which melting occurs depend on the dimensions of the particles and their velocity in the plasma flow (Fig. 5). It can be seen from the figure that the theoretical and experimental data obtained agree satisfactorily.

An improvement in the method of calculation and allowance for interaction between solid-phase particles and the effect of the solid phase on the gas phase will make it possible to obtain more accurate quantitative information on the parameters of two-phase jets.

#### NOTATION

$T$ , temperature, K;  $U$ , velocity, M/sec;  $C_D$ , drag coefficient;  $\gamma$ , density of flow components,  $\text{kg}/\text{m}^3$ ;  $Re$ , Reynolds number;  $Pr$ , Prandtl number;  $M$ , Mach number;  $Nu$ , Nusselt number;  $\mu$ , absolute viscosity,  $(\text{N}\cdot\text{sec})/\text{m}^2$ ;  $c_p$ , heat capacity,  $\text{W}/\text{kg}\cdot\text{deg}$ ;  $r$ , particle radius, m;  $\delta$ , particle diameter, m;  $f_N$ , density of particle distribution by size,  $\%/\mu\text{m}$ ;  $x$ , running coordinate, m;  $\alpha$ , heat-transfer coefficient;  $a_{av}$ , speed of sound, m/sec;  $r_0$ , radius of nozzle, m. Indices: p, parameters of the disperse phase; g, gas parameters; 0, initial parameters of the gas and disperse phase.

#### LITERATURE CITED

1. A. P. Iskrenkov et al., Heat and Mass Transfer at High Temperatures [in Russian], Minsk (1973), pp. 3-11.
2. F. B. Yurevich, V. V. Chuprasov, A. N. Filonenko, et al., Inventor's Certificate No. 1247662, Byull. Izobret., No. 28 (1986).
3. N. N. Yanenko et al., Supersonic Two-Phase Flows with High-Speed Particle Disequilibrium [in Russian], Novosibirsk (1980).
4. E. V. Kudryavtsev et al., Nonsteady Heat Transfer, Moscow (1961).
5. G. N. Abramovich, Turbulent Free Jets of Liquids and Gases [in Russian], Moscow (1948).
6. A. S. Strogii, "Study of the parameters of plasma jets and the effect of their transience on heat transfer with a barrier," Preprint, IMO AN Belorussian SSR, No. 18, Minsk (1982).